Desalination and Water Treatment
www.deswater.com

doi: 10.5004/dwt.2017.0124

62 (2017) 145–154
February

Response of aerobic granules and flocs on thiamethoxam inhibition. Part 2: Dual-morphology modelling and microbial distributions

Shuai Zhang[a], Kuizu Su[a,*], Dingding Chen[a], Shaogen Liu[b]

[a]*Department of Civil Engineering, Hefei University of Technology, Hefei 230009, China, Tel. +86 15555158791; email: 1512254643@qq.com (S. Zhang); Tel. +86 551 62905853; email: sukz@hfut.edu.cn (K. Su); Tel. +86 13856003291; email: cdd19910205@163.com (D. Chen)*
[b]*School of Environment and Energy Engineering, Anhui Jianzhu University, Hefei 230601, China, Tel. +86 13966667882; email: liushgen@mail.ustc.edu.cn*

Received 28 January 2016; Accepted 16 July 2016

ABSTRACT

The performance of aerobic granular sludge (AGS) and aerobic flocculent sludge (AFS) under toxicant inhibition was compared in the treatment of synthetic wastewater in an accompanying paper. A dual-morphology and multi-bacteria model based on activated sludge model No. 3 (ASM3) is developed to explain the inhibitory effect of toxic substances on the performance of AGS and AFS in this article. In this model, diffusion, storage and growth, endogenous respiration, and biomass decay are taken into account. The model is successfully validated with the oxygen uptake rate profiles for the aerobic granules in treating synthetic wastewater. The model simulation indicates that AGS showed high persistence against the toxic effects compared with AFS. The modeling results explicitly show that the oxygen and toxicant penetration depths in the granules play a crucial role in persistence against toxic effects. In addition, the model was used to simulate the distributions of microbial populations in AGS. The autotrophs are mainly present in the secondary outer layer of granules, and the toxic-degrading bacteria are mainly located in the outer layers, whereas the ordinary heterotrophs occupy the granule center, with only a small amount in the outer layers.

Keywords: Activated sludge model No. 3; Aerobic granular sludge; Aerobic flocculent sludge; Inhibition

1. Introduction

Aerobic granular sludge (AGS) is considered to be a special case of self-immobilized cells composed by biofilm. Compared with the conventional activated sludge, AGS has many advantages, such as high biomass retention, excellent settleability, dense and strong microbial structure, and the ability to withstand high organic loading [1]. AGS has been applied to the treatment of various industrial wastewaters, such as those of dairy [2], soybean-processing [3], and slaughterhouses [4], as well as toxic contaminations [5–7]. These results indicate that it is possible to use aerobic granules in treating toxic organic compounds. However, little information can be found on direct comparative studies between the tolerance to toxicity of AGS and aerobic flocculent sludge (AFS).

Mathematical modeling is a very useful tool for studying complex processes in the activated sludge wastewater treatment system. Model simulation and prediction can help us understand the reaction mechanism of biological treatment systems. Su and Yu [8] developed a generalized model for simulating an aerobic granule-based sequencing batch reactor (SBR) with considerations of biological processes, reactor hydrodynamics, mass transfer, and diffusion. A mathematical model established by de Kreuk et al. [9] can be used to describe an AGS reactor, capable of simultaneously removing chemical oxygen demand (COD), nitrogen and phosphate

* Corresponding author.

in a SBR. Ni and Yu [10] developed a model to describe the storage and growth activities of denitrifiers in aerobic granules under anoxic conditions. Kagawa et al. [11] developed a model for nutrient removal in an AGS system by coupling a reactor-scale model and a granule-scale model. However, a mathematical model of the removal and inhibition mechanisms of toxic substances by AGS and AFS is still limited.

The comparison between AGS and AFS in physical, chemical and biological characteristics is of major practical importance [12–14]. Rafiee et al. [12] investigated the 4-chlorophenol inhibition of flocculent and granular sludge SBR treating synthetic industrial wastewater. They observed that aerobic granules showed high persistence against the toxic effects of the xenobiotic compound. Lourenço et al. [13] compared AGS and flocculent SBR technologies for textile wastewater treatment. They found a better performance of the AGS SBR compared with AFS SBR, with respect to detoxification potential. These results are in agreement with those in the accompanying paper.

Therefore, the main objective of this work is to establish a mathematical model with inhibition kinetics, based on activated sludge model No. 3 (ASM3). The model was extended to two different biomass morphotypes (flocs and granules) and multiple microorganisms (autotrophs, ordinary heterotrophs and toxicant degrading bacteria). This model is used to describe the inhibitory and toxic effects of thiamethoxam (TMX) on AGS and AFS. The model can provide useful information on the treatment of toxic and refractory wastewater.

2. Materials and methods

Aerobic granules were cultivated as described in the accompanying paper. The batch experiments of COD removal by AGS and AFS at different TMX concentrations in the accompanying paper were used for model calibration. The measured oxygen uptake rate (OUR) profiles for the aerobic granules were used for model validation. In the OUR experiments, the granules were sampled from the SBR and washed twice, aerated them continuously to remove the external substrate. Then, the granules were transferred to 250 mL Erlenmeyer flasks. Two sets of batch tests (TMX concentrations were 0 and 100 mg L^{-1}) were conducted in this work. The mixed liquid suspended solids (MLSS) was kept at approximately 6.0 g L^{-1}, and the initial COD, NH_4^+–N, and phosphorus concentrations were 1,000, 50 and 10 mg L^{-1}, respectively. The dissolved oxygen (DO) concentration was measured with a DO electrode (LDO101, HACH Gmbh, Loveland, Colorado). The OUR was determined as the rate of change in measured DO concentration with respect to time using linear regression.

Kinetic and stoichiometric parameters in this model are shown in Table 1. The TMX inhibition coefficient, substrate saturation coefficient and storage rate constant were calibrated by the batch experiments, whereas the heterotrophic storage yield coefficient, the heterotrophic yield, the autotrophic yield, maximum growth rate and decay coefficient were determined as described by Gujer et al. [15]. The model was implemented in a combination of MATLAB code (ver. 2009a, MathWorks, Natick, MA) as the main algorithm driver.

3. Model development

3.1. Conceptual basis

The model is proposed to describe the inhibitory effect of TMX on the COD removal rate of AGS and AFS. The model

Table 1
Kinetic and stoichiometric coefficients used in the established model

Parameter	Definition	Values	Unit	Sources
Stoichiometry				
Y_{STO,O_2}	Aerobic yield of stored product per S_S	0.85	g COD g^{-1} COD	[15]
Y_{STO,NO_X}	Anoxic yield of stored product per S_S	0.80	g COD g^{-1} COD	[15]
Y_{H,O_2}	Aerobic yield of ordinary heterotrophic biomass	0.63	g COD g^{-1} COD	[15]
Y_{H,NO_X}	Anoxic yield of ordinary heterotrophic biomass	0.54	g COD g^{-1} COD	[15]
Y_A	Yield of autotrophic biomass per NO_3^-–N	0.24	g COD g^{-1} COD	[15]
f_{X_I}	Fraction of X_I in respiration	0.20	g COD g^{-1} COD	[15]
i_{N,S_S}	N content of S_S	0.03	g N g^{-1} COD	[15]
i_{N,X_I}	N content of X_I	0.02	g N g^{-1} COD	[15]
$i_{N,BM}$	N content of biomass, X_H, X_A	0.07	g N g^{-1} COD	[15]
Y_{T,STO,O_2}	Aerobic yield of stored product per S_T	0.85	g COD g^{-1} COD	[15]
Y_{T,STO,NO_X}	Anoxic yield of stored product per S_T	0.80	g COD g^{-1} COD	[15]
Y_{T,O_2}	Aerobic yield of TMX degrading biomass	0.63	g COD g^{-1} COD	[15]
Y_{T,NO_X}	Anoxic yield of TMX degrading biomass	0.54	g COD g^{-1} COD	[15]

(Continued)

Table 1 (*Continued*)

Parameter	Definition	Values	Unit	Sources
Kinetics				
Ordinary heterotrophic organisms, denitrification, X_H				
k_{STO}	Storage rate constant of X_H	30	d^{-1}	Determined
η_{NO_x}	Anoxic reduction factor of X_H	0.6	—	[15]
K_{O_2}	Saturation constant for S_{O_2} of X_H	0.2	g O_2 m^{-3}	[15]
K_{NO_x}	Saturation constant for S_{NO_x} of X_H	0.5	g N m^{-3}	[15]
K_S	Saturation constant for substrate S_S of X_H	400	g COD m^{-3}	Determined
K_{STO}	Saturation constant for X_{STO} of X_H	1.0	g COD g^{-1} COD	[15]
μ_H	Maximum growth rate of X_H	2.0	d^{-1}	[15]
K_{NH_4}	Saturation constant for ammonium, S_{NH_4} of X_H	0.01	g N m^{-3}	[15]
b_{H,O_2}	Aerobic endogenous respiration rate of X_H	0.2	d^{-1}	[15]
b_{H,NO_x}	Anoxic endogenous respiration rate of X_H	0.1	d^{-1}	[15]
b_{STO,O_2}	Aerobic respiration rate for X_{STO}	0.2	d^{-1}	[15]
b_{STO,NO_x}	Anoxic respiration rate for X_{STO}	0.1	d^{-1}	[15]
Autotrophic organisms, nitrification, X_A				
μ_A	Maximum growth rate of X_A	1.0	d^{-1}	[15]
K_{A,NH_4}	Ammonium substrate saturation for X_A	1.0	g N m^{-3}	[15]
K_{A,O_2}	Oxygen saturation for nitrifiers	0.5	g O_2 m^{-3}	[15]
b_{A,O_2}	Aerobic endogenous respiration rate of X_A	0.15	d^{-1}	[15]
b_{A,NO_x}	Anoxic endogenous respiration rate of X_A	0.05	d^{-1}	[15]
TMX degrading organisms, denitrification, X_T				
$k_{T,STO}$	Storage rate constant of X_T	25	d^{-1}	Determined
η_{T,NO_x}	Anoxic reduction factor of X_T	0.6	—	[15]
K_{T,O_2}	Saturation constant for S_{O_2} of X_T	0.2	g O_2 m^{-3}	[15]
$K_{T,NOx}$	Saturation constant for S_{NO_x} of X_T	0.5	g N m^{-3}	[15]
K_T	Saturation constant for substrate S_T of X_T	5.0	g COD m^{-3}	Determined
$K_{T,STO}$	Saturation constant for $X_{T,STO}$ of X_T	1.0	g COD g^{-1} COD	[15]
μ_T	Maximum growth rate of X_T	2.0	d^{-1}	[15]
K_{T,NH_4}	Saturation constant for ammonium, S_{NO_x} of X_T	0.01	g N m^{-3}	[15]
b_{T,O_2}	Aerobic endogenous respiration rate of X_T	0.2	d^{-1}	[15]
b_{T,NO_x}	Anoxic endogenous respiration rate of X_T	0.1	d^{-1}	[15]
b_{T,STO,O_2}	Aerobic respiration rate for $X_{T,STO}$	0.2	d^{-1}	[15]
b_{T,STO,NO_x}	Anoxic respiration rate for $X_{T,STO}$	0.1	d^{-1}	[15]
K_I	TMX inhibition coefficient	90	mg L^{-1}	Determined
$D_e^{o_2}$	effective diffusivity of O_2	1.58×10^{-9}	m^2 s^{-1}	[8]
D_e^{TMX}	effective diffusivity of TMX	2.0×10^{-10}	m^2 s^{-1}	Determined

developed in this work has 10 model components, as shown in Table 2. In this model, the toxic substance TMX and TMX degrading microorganisms were added. TMX degrading microorganisms are a special kind of heterotrophs and are grown by TMX as a single carbon source. The ordinary heterotrophic microorganisms represent the other heterotrophs except TMX degrading bacteria. The model mainly involves 19 microbial processes: the process of ordinary heterotrophic microorganisms including aerobic storage and anoxic storage, on S_S, aerobic growth and anoxic growth on X_{STO}, aerobic respiration and anoxic respiration of X_{STO}, aerobic endogenous respiration, and anoxic endogenous respiration; the process of autotrophic microorganisms including aerobic growth, aerobic endogenous respiration, and anoxic endogenous respiration; and the process of TMX degrading microorganisms including aerobic storage and anoxic storage on S_T, aerobic growth and anoxic growth on $X_{T,STO}$, aerobic respiration and anoxic respiration of $X_{T,STO}$, aerobic endogenous respiration, and anoxic endogenous respiration. A stoichiometric matrix for particulate and soluble components and expressions of the process rates in the model is outlined in Tables 3 and 4.

Table 2
Model components

Symbol	Definition	Symbol	Definition
S_{O_2}	Dissolved oxygen	X_H	Ordinary heterotrophic microorganisms
S_S	Readily biodegradable substrate	X_A	Autotrophic microorganisms
S_{NO_x}	Nitrate and nitrite	X_{STO}	Storage products of ordinary heterotrophic microorganisms
S_{NH_4}	Ammonium and ammonia – N	X_T	TMX degrading microorganisms
S_T	Thiamethoxam	$X_{T,STO}$	Storage products of TMX degrading microorganisms

Table 3
Stoichiometric matrix for particulate and soluble components

Bacteria	Process	Soluble components (mg L^{-1})					Particulate components (g m^{-3})				
		S_{O_2}	S_S	S_{NH_4}	S_{NO_x}	S_T	X_H	X_{STO}	X_A	X_T	$X_{T,STO}$
Ordinary heterotrophic organisms	Aerobic storage	$Y_{STO,O_2}-1$	–1	i_{N,S_S}				Y_{STO,O_2}			
	Anoxic storage		–1	i_{N,S_S}	$\frac{Y_{STO,NO_X}-1}{2.86}$			Y_{STO,NO_X}			
	Aerobic growth	$1-\frac{1}{Y_{H,O_2}}$		$-i_{N,BM}$			1	$-\frac{1}{Y_{H,O_2}}$			
	Anoxic growth			$-i_{N,BM}$	$\frac{Y_{H,NO_X}-1}{2.86Y_{H,NO_X}}$		1	$-\frac{1}{Y_{H,NO_X}}$			
	Aerobic endogenous respiration	$f_{X_I}-1$		$i_{N,BM}-f_{X_I}i_{N,X_I}$			–1				
	Anoxic endogenous respiration			$i_{N,BM}-f_{X_I}i_{N,X_I}$	$\frac{f_{X_I}-1}{2.86}$		–1				
	Aerobic respiration of X_{STO}	–1						–1			
	Anoxic respiration of X_{STO}				$-\frac{1}{2.86}$			–1			
Autotrophic organisms	Aerobic growth	$1-\frac{4.57}{Y_A}$		$-\frac{1}{Y_A}-i_{N,BM}$	$\frac{1}{Y_A}$				1		
	Aerobic endogenous respiration	$f_{X_I}-1$		$i_{N,BM}-f_{X_I}i_{N,X_I}$					–1		
	Anoxic endogenous respiration			$i_{N,BM}-f_{X_I}i_{N,X_I}$	$\frac{f_{X_I}-1}{2.86}$				–1		

(Continued)

Table 3 (*Continued*)

Bacteria	Process	Soluble components (mg L^{-1})					Particulate components (g m^{-3})				
		S_{O_2}	S_S	S_{NH_4}	S_{NO_x}	S_T	X_H	X_{STO}	X_A	X_T	$X_{T,STO}$
TMX degrading organisms	Aerobic storage	$Y_{T,STO,O_2}-1$		i_{N,S_S}		–1					Y_{T,STO,O_2}
	Anoxic storage			i_{N,S_S}	$\frac{Y_{T,STO,NO_X}-1}{2.86}$	–1					Y_{T,STO,NO_X}
	Aerobic growth	$1-\frac{1}{Y_{T,O_2}}$		$-i_{N,BM}$						1	$-\frac{1}{Y_{T,O_2}}$
	Anoxic growth			$-i_{N,BM}$	$\frac{Y_{T,NO_X}-1}{2.86Y_{T,NO_X}}$					1	$-\frac{1}{Y_{T,NO_X}}$
	Aerobic endogenous respiration	$f_{X_I}-1$		$i_{N,BM}-f_{X_I}i_{N,X_I}$						–1	
	Anoxic endogenous respiration			$i_{N,BM}-f_{X_I}i_{N,X_I}$	$\frac{f_{X_I}-1}{2.86}$					–1	
	Aerobic respiration of $X_{T,STO}$	–1									–1
	Anoxic respiration of $X_{T,STO}$				$-\frac{1}{2.86}$						–1

Table 4
Expressions of the process rates

Bacteria	Process	Kinetics rates expressions
Ordinary heterotrophic organisms	Aerobic storage	$k_{STO}\left(\frac{K_I}{K_I+S_T}\right)\left(\frac{S_{O_2}}{K_{O_2}+S_{O_2}}\right)\left(\frac{S_S}{K_S+S_S}\right)X_H$
	Anoxic storage	$k_{STO}\eta_{NO_X}\left(\frac{K_I}{K_I+S_T}\right)\left(\frac{K_{O_2}}{K_{O_2}+S_{O_2}}\right)\left(\frac{S_{NO_X}}{K_{NO_X}+S_{NO_X}}\right)\left(\frac{S_S}{K_S+S_S}\right)X_H$
	Aerobic growth	$\mu_H\left(\frac{K_I}{K_I+S_T}\right)\left(\frac{S_{O_2}}{K_{O_2}+S_{O_2}}\right)\left(\frac{S_{NH_4}}{K_{NH_4}+S_{NH_4}}\right)\left(\frac{X_{STO}/X_H}{K_{STO}+X_{STO}/X_H}\right)X_H$
	Anoxic growth	$\mu_H\eta_{NO_X}\left(\frac{K_I}{K_I+S_T}\right)\left(\frac{K_{O_2}}{K_{O_2}+S_{O_2}}\right)\left(\frac{S_{NO_X}}{K_{NO_X}+S_{NO_X}}\right)\left(\frac{S_{NH_4}}{K_{NH_4}+S_{NH_4}}\right)\left(\frac{X_{STO}/X_H}{K_{STO}+X_{STO}/X_H}\right)X_H$
	Aerobic endogenous respiration	$b_{H,O_2}\left(\frac{S_{O_2}}{K_{O_2}+S_{O_2}}\right)X_H$
	Anoxic endogenous respiration	$b_{H,NO_X}\left(\frac{K_{O_2}}{K_{O_2}+S_{O_2}}\right)\left(\frac{S_{NO_X}}{K_{NO_X}+S_{NO_X}}\right)X_H$
	Aerobic respiration of X_{STO}	$b_{STO,O_2}\left(\frac{S_{O_2}}{K_{O_2}+S_{O_2}}\right)X_{STO}$
	Anoxic respiration of X_{STO}	$b_{STO,NO_X}\left(\frac{K_{O_2}}{K_{O_2}+S_{O_2}}\right)\left(\frac{S_{NO_X}}{K_{NO_X}+S_{NO_X}}\right)X_{STO}$

(Continued)

Table 4 (*Continued*)

Bacteria	Process	Kinetics rates expressions
Autotrophic organisms	Aerobic growth	$\mu_A\left(\frac{K_I}{K_I+S_T}\right)\left(\frac{S_{O_2}}{K_{A,O_2}+S_{O_2}}\right)\left(\frac{S_{NH_4}}{K_{A,NH_4}+S_{NH_4}}\right)X_A$
	Aerobic endogenous respiration	$b_{A,O_2}\left(\frac{S_{O_2}}{K_{A,O_2}+S_{O_2}}\right)X_A$
	Anoxic endogenous respiration	$b_{A,NO_X}\left(\frac{K_{O_2}}{K_{A,O_2}+S_{O_2}}\right)\left(\frac{S_{NO_X}}{K_{A,NO_X}+S_{NO_X}}\right)X_A$
TMX degrading organisms	Aerobic storage	$k_{T,STO}\left(\frac{S_{O_2}}{K_{T,O_2}+S_{O_2}}\right)\left(\frac{S_T}{K_T+S_T+S_T^2/K_I}\right)X_T$
	Anoxic storage	$k_{T,STO}\eta_{T,NO_X}\left(\frac{K_{O_2}}{K_{T,O_2}+S_{O_2}}\right)\left(\frac{S_{NO_X}}{K_{T,NO_X}+S_{NO_X}}\right)\left(\frac{S_T}{K_T+S_T+S_T^2/K_I}\right)X_T$
	Aerobic growth	$\mu_T\left(\frac{S_{O_2}}{K_{T,O_2}+S_{O_2}}\right)\left(\frac{S_{NH_4}}{K_{T,NH_4}+S_{NH_4}}\right)\left(\frac{X_{T,STO}/X_T}{K_{T,STO}+X_{T,STO}/X_T}\right)X_T$
	Anoxic growth	$\mu_T\eta_{T,NO_X}\left(\frac{K_{O_2}}{K_{T,O_2}+S_{O_2}}\right)\left(\frac{S_{NO_X}}{K_{T,NO_X}+S_{NO_X}}\right)\left(\frac{S_{NH_4}}{K_{T,NH_4}+S_{NH_4}}\right)\left(\frac{X_{T,STO}/X_T}{K_{T,STO}+X_{T,STO}/X_T}\right)X_T$
	Aerobic endogenous respiration	$b_{T,O_2}\left(\frac{S_{O_2}}{K_{T,O_2}+S_{O_2}}\right)X_T$
	Anoxic endogenous respiration	$b_{T,NO_X}\left(\frac{K_{O_2}}{K_{T,O_2}+S_{O_2}}\right)\left(\frac{S_{NO_X}}{K_{T,NO_X}+S_{NO_X}}\right)X_T$
	Aerobic respiration of $X_{T,STO}$	$b_{T,STO,O_2}\left(\frac{S_{O_2}}{K_{T,O_2}+S_{O_2}}\right)X_{T,STO}$
	Anoxic respiration of $X_{T,STO}$	$b_{T,STO,NO_X}\left(\frac{K_{O_2}}{K_{T,O_2}+S_{O_2}}\right)\left(\frac{S_{NO_X}}{K_{T,NO_X}+S_{NO_X}}\right)X_{T,STO}$

3.2. Diffusion of components

For all of the components involved in the biochemical reactions, the first step is their diffusion into the interior of granules before the reaction. Thus, the concentrations of the components at different distances from the center of the granule are also very different. In this model the granules are sliced up, and the concentration of each slice is regarded as constant. The mass balance of component *i* for a slice of one granule can be written as follows [8]:

$$\frac{\partial S^i}{\partial t}=\frac{\partial^2 S^i}{\partial r^2}+\frac{2}{r}\cdot\frac{\partial S^i}{\partial r}\pm\frac{k^i}{D_e^i} \tag{1}$$

with boundary conditions:

$$S^i=S^i_{sur},\quad r=R$$
$$\frac{\partial S^i}{\partial r}=0,\quad r=\delta^i$$

where δ^i is the penetration depth of component *i* into the granule, in which the gradient of the component concentration vanishes by symmetry, and *r* is the distance of the slice from the granule center.

3.3. Inhibition kinetics

The Monod model described the growth of microorganisms under the single substrate. In the presence of toxic substances, microbial growth will be inhibited, so the modified Monod model was used. As a type of toxic refractory substance, TMX has a noncompetitive inhibition effect on the growth of microorganisms in the granular sludge, and the kinetic expression is described as follows [16]:

$$r_S=\frac{\mu_{max}S}{(K+S)\left(1+\frac{S_T}{K_I}\right)} \tag{2}$$

where μ_{max} is the maximum specific growth rate; K_I is the inhibition coefficient; S is the substrate concentration; S_T is the TMX concentration; and K is the saturation constant for substrate S.

In addition, the TMX degrading microorganisms in the reactor that utilize TMX as a single substrate for growth will engender substrate inhibition, and the kinetic expression is as follows [16]:

$$r_T = \frac{\mu_T S_T}{K_T + S_T + \frac{S_T^2}{K_I}} \quad (3)$$

where μ_T is the maximum specific growth rate of the TMX degrading microorganisms, and K_T is the saturation constant for substrate S_T.

4. Results and discussion

4.1. Model calibration and validation

The model calibration is based on a comparison between the model predictions and the experimental results with the same input model parameters. In the experiments, COD concentrations in the influent remained at 1,000 mg L^{-1}. The results of batch experiments and the corresponding model predictions are illustrated in Fig. 1. The TMX inhibition coefficient was calibrated by the batch experiment, and the value is determined to be 90 mg L^{-1}.

As shown in Fig. 1, although the COD removal rate decreased as the TMX concentrations increased from 0 to 500 mg L^{-1}, and the COD removal efficiency of AGS was higher than that of AFS. In addition, with the increase in the TMX concentration, the superiority of AGS is more obvious. When the TMX concentration reached 500 mg L^{-1}, the COD removal rate of AGS could remain at 57.8%, while that of AFS only reached approximately 20%. In general, the ability to bear the TMX toxicity of AGS is better than that of AFS. This is in accordance with the experimental results of Uygur and Kargi [17] and Rafiee et al. [12]. They found that aerobic granules, in comparison with suspended flocs, showed high persistence against the toxic effects of the xenobiotic compound.

Experimental data of the OUR at the TMX concentrations were 0 and 100 mg L^{-1} are employed for model verification. The simulating results are shown in Fig. 2. Two different phases can be distinguished in the OUR profiles. The first phase (high OUR) is related to the consumption of external substrate, while the second phase (low OUR) corresponds to the storage polymer production consumption [18]. Moreover, the OUR was decreased distinctly in the presence of TMX. The good agreement between the experimental and simulated results suggests the validity of the model established in this work.

4.2. Model simulation of oxygen and TMX diffusion

The oxygen penetration depth in aerobic granules plays a crucial role in the conversion rates of different components and thus on the overall nutrient removal efficiency [9]. As a type of toxic refractory substance, the TMX penetration depth is also important, directly affecting the inhibitory effect. The simulated oxygen concentration profiles in aerobic granules are shown in Fig. 3(A). For flocs and granules with a radius less than 0.50 mm, oxygen can diffuse into the center of the granules. For granules, oxygen diffusion is the limiting step for oxygen utilization, and the microbial reaction rate decreases due to the low oxygen concentration in the interior of granules [19]. The simulated TMX concentration profiles in aerobic granules are shown in Fig. 3(B). For 1.5 mm granules, the TMX concentration decreases to 0 at 1.0 mm from the surface; for smaller AGS and AFS, TMX can diffuse into the granules center. Fig. 3(C) shows the simulated TMX profiles at different concentrations. The TMX diffusion in the granules is obviously restricted. When the TMX concentration is 500 mg L^{-1}, it can just diffuse into the center of the granules, and the restriction of TMX diffusion reached a maximum. The TMX inhibition in the outer layers is stronger than in the center of the granules. However, there is no limitation

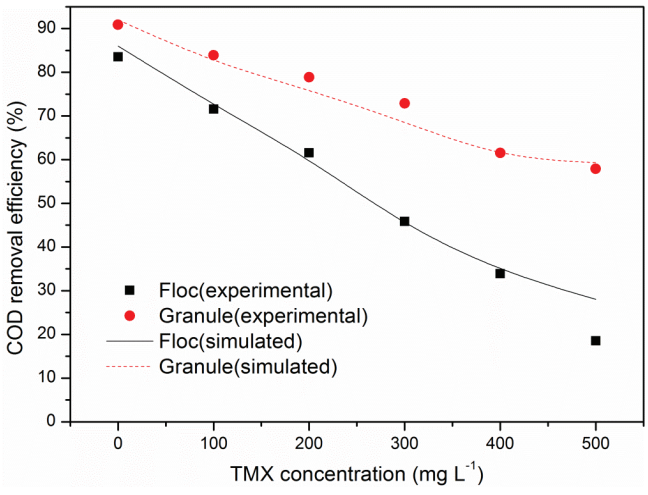

Fig. 1. Model calibration results of the COD removal efficiency for AFS and AGS during the treatment of synthetic wastewater in the presence of TMX.

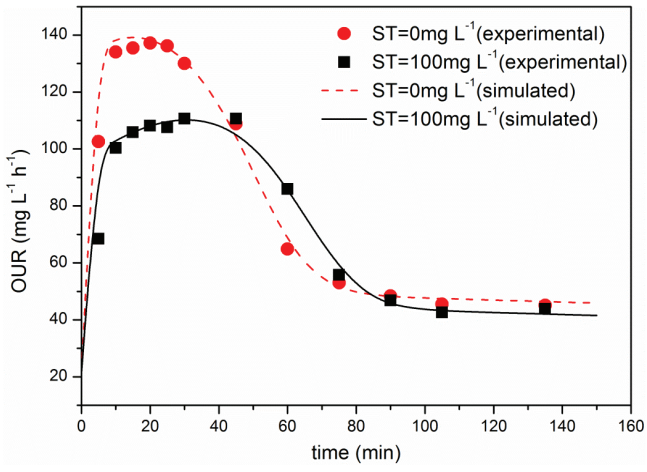

Fig. 2. Model validation results of the OUR profiles for the aerobic granules in treating synthetic wastewater.

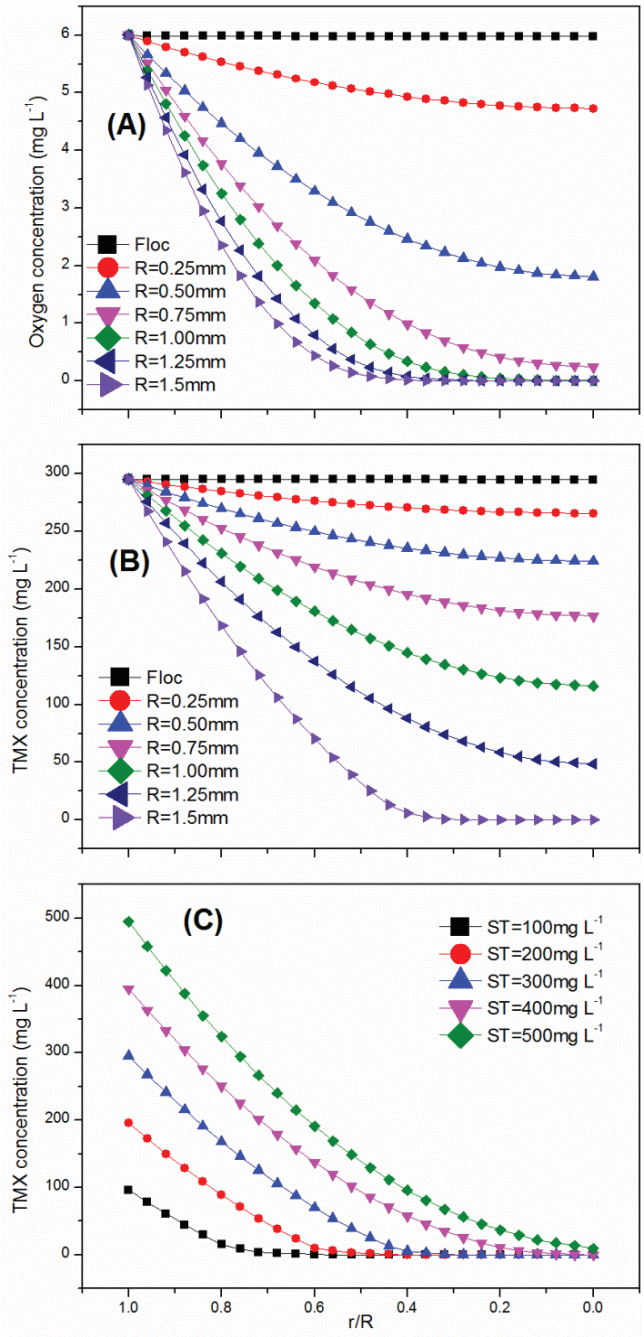

Fig. 3. Model simulation results of: (A) Oxygen concentration profiles (DO = 6 mg L^{-1}); (B) TMX concentration profiles (TMX = 300 mg L^{-1}) of AFS and AGS with different particle sizes; and (C) TMX at different concentrations profiles of AGS (radius = 1.5 mm).

of diffusion of AFS. These results support the phenomenon that the COD removal rate of AFS decreased sharply and that of AGS fell slowly in Fig. 1. The ability to tolerate the TMX toxicity of AGS is better than that of AFS [12].

To understand how the diffusion of oxygen and TMX affect the COD removal rate, this study simulated the COD

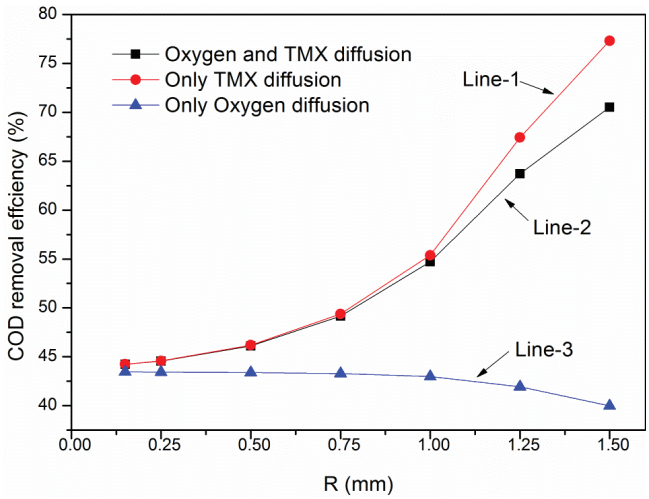

Fig. 4. Model simulation results of the COD removal efficiency for AFS and AGS with different particle sizes. Line-1: DO = 6 mg L^{-1}, TMX diffusion; Line-2: DO and TMX diffusion; Line-3: DO diffusion, TMX = 300 mg L^{-1}.

removal rate for AFS and AGS with different particle sizes, considering the TMX diffusion or oxygen diffusion, respectively, and considering the diffusion of both oxygen and TMX (Fig. 4). Line-1 (only TMX diffusion) and Line-2 (diffusion of both oxygen and TMX) are relatively close, which indicates that the influence of oxygen diffusion on the COD removal rate is relatively weak under toxicant inhibition. Line-3 (only oxygen diffusion) showed a downward trend, and has a larger gap with Line-2. This shows that the small granules and flocs are superior to large granules at COD removal when there is no effect from TMX diffusion, and TMX diffusion has a great influence on the COD removal rate. With the increase in the size of granules, the limitation of TMX diffusion becomes more obvious, and it was possible that the granules' special structure provided protection against the diffusive toxins. The large granules are dominant on the COD removal under toxicant inhibition. The oxygen diffusion limitation is adverse to the COD removal, whereas the TMX diffusion limitation benefits the COD removal and plays a leading role in this process.

4.3. Model simulation of microbial specific growth rate

The effects of bioparticle size and TMX on the microbial growth in aerobic granules, expressed as the microbial specific growth rate, were further investigated (Fig. 5). When there is no TMX inhibition, the autotrophs have to grow under oxygen-diffusion-limitation conditions, which slows the nitrification process [20]. The ordinary heterotrophs can grow in the granule center by using NO_3^-–N as the electron acceptor, and they can also grow on the outer layers, where they use DO as an electron acceptor [21]. In addition, the oxygen saturation constant of ordinary heterotrophs is relatively low. Therefore, the specific growth rate of autotrophs in the granules center is almost zero, whereas ordinary heterotrophs have a higher specific growth rate in the granules center and outer layers. In the presence of TMX, the specific

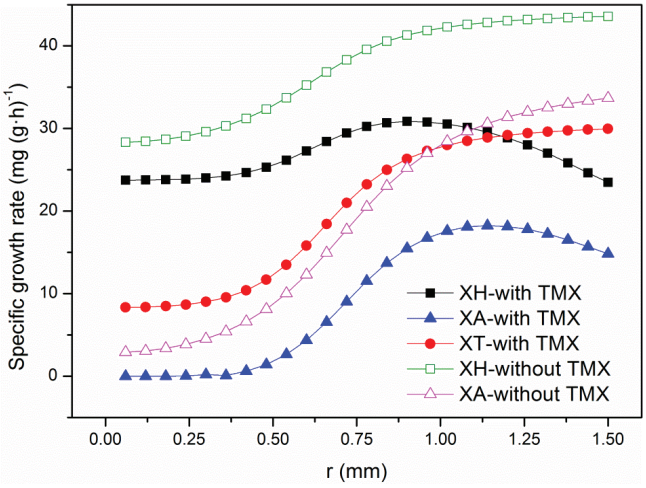

Fig. 5. Model simulation of the specific growth rate as a function of the radius (r) of the aerobic granules.

growth rate is mainly affected by TMX diffusion. In the outer layer of granules, the specific growth rate of autotrophs and ordinary heterotrophs decreased due to TMX inhibition. With an increase in the distance from the granules center, for autotrophs or ordinary heterotrophs, the gap of the specific growth rate between treatments with and without TMX becomes larger. This shows that as the distance from the center of granules increases, the TMX inhibition becomes stronger.

4.4. Microbial population distribution in the aerobic granules

Due to the difference in the specific growth rates, the microbial distributions in the granules are also different. The model simulated the microbial population distribution in AGS after 30 d, as shown in Fig. 6. The AGS radius is 1.5 mm in the SBR reactor; biomass growing beyond this limit is removed by detachment [22]. The initial concentration of X_H is 700 g m^{-3}; X_A is 150 g m^{-3}; X_T is 150 g m^{-3}; and the microorganisms are uniformly distributed within the granules in the initial state. The simulated TMX degrading bacteria distribution is illustrated in Fig. 6(A). TMX degrading bacteria were grown by TMX as a single substrate, and TMX mainly exists in the outer layer of granules. Therefore, the TMX degrading bacteria were mainly located in the outer layers. The autotrophs have a higher oxygen saturation constant and have to grow only on the outer layers of the aerobic granules to meet their essential requirements for DO. However, because of the intensive inhibition by TMX in the outermost layers, the autotrophs are mainly distributed in the secondary outer layer of granules (Fig. 6(B)). Although the ordinary heterotrophs can grow well in aerobic and anoxic conditions, the outer layer of granules has a stronger TMX inhibition. Therefore, the ordinary heterotrophs occupy the granule center, and there is only a small amount in the outer layers (Fig. 6(C)). The similar results for the microbial population distribution in aerobic granules is also reported by Beun et al. [23].

Compared with the loose AFS, the compact structure and large size of AGS protect the microbes within granules from toxic inhibition. However, there is no oxygen diffusion limitation in AFS, which exist in AGS. Therefore, AGS has a good potential in treating toxic and refractory wastewater, and AFS is more suitable for the treatment of non-toxic wastewater.

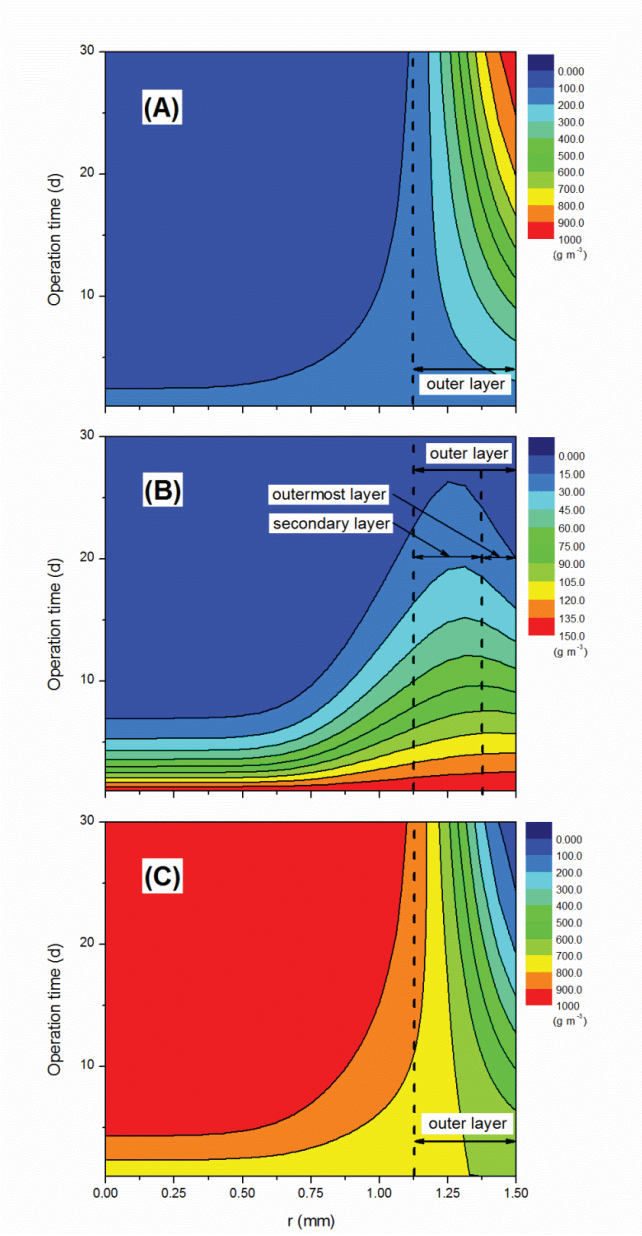

Fig. 6. Model simulation of microbial population distribution in the aerobic granules: (A) TMX degrading microorganisms; (B) autotrophic microorganisms; and (C) ordinary heterotrophic microorganisms.

5. Conclusions

In this study, a dual-morphology and multi-bacteria model is developed to describe the inhibitory effect of TMX on the COD removal rate of AGS and AFS in the treatment

of simulated wastewater. ASM3 was modified with the toxic substance TMX, and biochemical reactions under aerobic and anoxic conditions, including hydrolysis, storage and growth, endogenous respiration, and biomass decay, were taken into account. The validity of the model is verified with the OUR, and the results show that TMX has a significant inhibition effect on the OUR for the aerobic granules. The model simulation indicates that AGS, in comparison with AFS, showed high persistence against the toxic effects of the xenobiotic compound TMX. The TMX diffusion limitation is a benefit to COD removal and plays a leading role in this process. The compact structure of granules is a protection barrier against the diffusive toxins of TMX. The large granules have a good potential for treating toxic wastewater. In addition, the autotrophs are mainly located in the secondary outer layers of granules, and the TMX degrading bacteria are mainly located in the outer layer of granules, whereas the ordinary heterotrophs occupy the center of the granules and are in the outer layers only in small amounts.

Acknowledgements

This work was supported by the National Natural Science Foundation of China (Grant numbers 51378165 and 51278002).

References

[1] S.S. Adav, D.J. Lee, K.Y. Show, J.H. Tay, Aerobic granular sludge: recent advances, Biotechnol. Adv., 26 (2008) 411–423.
[2] C. Bumbac, I.A. Ionescu, O. Tiron, V.R. Badescu, Continuous flow aerobic granular sludge reactor for dairy wastewater treatment, Water Sci. Technol., 71 (2015) 440–445.
[3] Z. Su, H.Q. Yu, Formation and characterization of aerobic granules in a sequencing batch reactor treating soybean-processing wastewater, Environ. Sci. Technol., 39 (2005) 2818–2827.
[4] Y. Liu, X. Kang, L. Xin, Y. Yuan, Performance of aerobic granular sludge in a sequencing batch bioreactor for slaughterhouse wastewater treatment, Bioresour. Technol., 190 (2015) 487–491.
[5] M. Jian, C. Tang, M. Liu, Adsorptive removal of Cu^{2+} from aqueous solution using aerobic granular sludge, Desal. Wat. Treat., 54 (2015) 2005–2014.
[6] Y. Zhang, J. Tay, Toxic and inhibitory effects of trichloroethylene aerobic co-metabolism on phenol-grown aerobic granules, J. Hazard. Mater., 286 (2015) 204–210.
[7] Y.V. Nancharaiah, G. Kiran Kumar Reddy, T.V. Krishna Mohan, V.P. Venugopalan, Biodegradation of tributyl phosphate, an organosphate triester, by aerobic granular biofilms, J. Hazard. Mater., 283 (2015) 705–711.
[8] K.Z. Su, H.Q. Yu, A generalized model for aerobic granule-based sequencing batch reactor. 1. Model development, Environ. Sci. Technol., 40 (2006) 4703–4708.
[9] M.K. de Kreuk, C. Picioreanu, M. Hosseini, J.B. Xavier, M.C.M. van Loosdrecht, Kinetic model of a granular sludge SBR: influences on nutrient removal, Biotechnol. Bioeng., 97 (2007) 801–815.
[10] B.J. Ni, H.Q. Yu, Storage and growth of denitrifiers in aerobic granules: Part I. Model development, Biotechnol. Bioeng., 99 (2008) 314–323.
[11] Y. Kagawa, J. Tahata, N. Kishida, S. Matsumoto, C. Picioreanu, M.C.M. van Loosdrecht, S. Tsuneda, Modeling the nutrient removal process in aerobic granular sludge system by coupling the reactor- and granule-scale models, Biotechnol. Bioeng., 112 (2015) 53–64.
[12] M. Rafiee, A. Mesdaghinia, M.H. Ghahremani, S. Nasseri, R. Nabizadeh, 4-Chlorophenol inhibition on flocculent and granular sludge sequencing batch reactors treating synthetic industrial wastewater, Desal. Wat. Treat., 49 (2012) 307–316.
[13] N.D. Lourenço, R.D.G. Franca, M.A. Moreira, F.N. Gil, C.A. Viegas, H.M. Pinheiro, Comparing aerobic granular sludge and flocculent sequencing batch reactor technologies for textile wastewater treatment, Biochem. Eng. J., 104 (2015) 57–63.
[14] S.B. Sam, E. Dulekgurgen, Characterization of exopolysaccharides from floccular and aerobic granular activated sludge as alginate-like-exoPS, Desal. Wat. Treat., 57 (2016) 2534–2545.
[15] W. Gujer, M. Henze, T. Mino, M. Vanloosdrecht, Activated sludge model No. 3, Water Sci. Technol., 39 (1999) 183–193.
[16] M. Henze, M.C.M. van Loosdrecht, G.A. Ekama, D. Brdjanovic, Biological Wastewater Treatment: Principles, Modeling and Design, IWA, London, 2008.
[17] A. Uygur, F. Kargi, Phenol inhibition of biological nutrient removal in a four-step sequencing batch reactor, Process Biochem., 39 (2004) 2123–2128.
[18] M.C.M. van Loosdrecht, M.A. Pot, J.J. Heijnen, Importance of bacterial storage polymers in bioprocesses, Water Sci. Technol., 35 (1997) 41–47.
[19] Z.C. Chiu, M.Y. Chen, D.J. Lee, C.H. Wang, J.Y. Lai, Oxygen diffusion and consumption in active aerobic granules of heterogeneous structure, Appl. Microbiol. Biotechnol., 75 (2007) 685–691.
[20] W.A.J. van Benthum, M.C.M. van Loosdrecht, J.J. Heijnen, Control of heterotrophic layer formation on nitrifying biofilms in a biofilm airlift suspension reactor, Biotechnol. Bioeng., 53 (1997) 397–405.
[21] B.J. Ni, H.Q. Yu, Y.J. Sun, Modeling simultaneous autotrophic and heterotrophic growth in aerobic granules, Water Res., 42 (2008) 1583–1594.
[22] J.B. Xavier, M.K. de Kreuk, C. Picioreanu, M.C.M. van Loosdrecht, Multi-scale individual-based model of microbial and bioconversion dynamics in aerobic granular sludge, Environ. Sci. Technol., 41 (2007) 6410–6417.
[23] J.J. Beun, J.J. Heijnen, M.C.M. van Loosdrecht, N-Removal in a granular sludge sequencing batch airlift reactor, Biotechnol. Bioeng., 75 (2001) 82–92.